Received: 8 February 2023 | Accepted: 5 April 2023

DOI: 10.1002/maco.202313786

ARTICLE

Materials and Corrosion

# Thermoset thin film primers: Influence of substrate, layer thickness and wettability of additives in laboratory testing

**Simon Wiener**[1,2] | **Bernhard Strauß**[1] | **Gerald Luckeneder**[1] | **Josef Hagler**[1] | **Markus Valtiner**[2]

[1]Voestalpine Stahl GmbH, Linz, Austria

[2]Institute of Applied Physics, Vienna University of Technology, Vienna, Austria

**Correspondence**
Simon Wiener, Voestalpine Stahl GmbH, Linz 4020, Austria.
Email: wiener.simon@gmail.com

**Funding information**
Österreichische Forschungsförderungsgesellschaft

**Abstract**

Steel sheets are often protected from corrosion using primers in combination with a top coat. However, the effectiveness of primers alone has not been extensively studied. Here, we use a selection of complementary corrosion tests for benchmarking the performance of thin-film primers across a set of varying engineering parameters such as thickness, wettability, and substrate. Five established tests were selected, covering all predominant mechanisms that may occur, namely tests for cathodic and anodic delamination and barrier protection. Electrochemical investigations, among others, were carried out to evaluate the corrosion behavior, while structural properties were analyzed using techniques such as SEM. A total of nine primer formulations were tested in a layer thickness range of 3–9 μm, on GI and ZM-coated steel. Both layer thickness and substrate strongly influence performance, and to a lesser degree the primer formulation. Further, hydrophobization has a beneficial effect on cathodic delamination, while white rust formation is enhanced due to pigment leaching limitations. This suggests that competing effects can be traced well using the combination of the suggested five tests.

**KEYWORDS**

anticorrosive pigments, coil coatings, corrosion protection, laboratory testing, thin film primer

## 1 | INTRODUCTION

Metals in all their shapes play a major role in today's economic system, as their processing and usage form the basis of many important sectors of the economy, such as the construction sector, the automotive sector, and the aviation sector to name just a few. These materials are not immune to environmental influence, more precisely corrosion. Industry is trying to address this problem in a number of ways, including the development of corrosion-resistant alloys or the usage of inorganic coatings, such as galvanizing in the case of steel.[1–3]

If these options are insufficient, it is also possible to convert the oxide layer on the surface of the substrate into a coating with altered properties. These thin, so-called conversation layers often consist of chromates or phosphates and are intended not only to provide

enhanced corrosion protection but also to improve adhesion for organic coatings such as paints and lacquers applied on top of them.[4,5]

Such organic coatings are typically used when particularly good corrosion protection is to be achieved or when special requirements are placed on the material. They consist of a large number of different components; in addition to binders and solvents, they normally also contain fillers, additives, and pigments. One type of contained pigment, the anticorrosion pigments, can be roughly divided into three categories depending on the mechanism of action—barrier pigments, sacrificial pigments, and inhibitive pigments. As a result, paint coatings primarily serve as a barrier to water, oxygen, and other corrosive chemical substances while also acting as a reservoir for corrosion inhibitors. Together, these two functions prevent corrosion on the metal substrate.[6–8]

To subsequently find out whether the selected coating system meets the requirements or, in the case of quality control, to check whether the samples have been manufactured and processed in accordance with the production standards, corrosion tests are usually carried out. Consequently, corrosion testing of organic coatings, especially with accelerated corrosion tests in the laboratory, has become an indispensable part of coating development. This evolution started more than 100 years ago, with the development of the salt spray test (SST) followed by temperature and humidity tests as well as the comparatively new cyclic corrosion tests, which has been pushed by the automotive industry in particular.[9,10]

Electrochemical testing is a common method used for corrosion testing, utilizing a wide range of electrochemical tests such as potentiodynamic or cyclic polarization tests. The development of electrochemical impedance spectroscopy (EIS) has been a significant milestone in this field, and it is extensively used today.[11]

The availability of electrochemical and technological testing methods has led to the development of countless modified and new tests since the beginning of corrosion testing. New tests continue to be developed with the aim of providing faster and more reliable tools for predicting the corrosion resistance of organic coatings. These tests are useful in facilitating the development of new coatings tailored to specific needs and enable a direct comparison of the performance of different coatings.

However, when attributing all these tests to the limited number of basic coating corrosion mechanisms—that is, anodic and cathodic delamination,[12–15] blistering,[16–19] water disbondment,[20,21] and filiform corrosion[22,23]—it turns out that a handful of carefully selected tests should be sufficient to obtain a comprehensive overview of the protection performance of organic coatings. The situation becomes much more complex when additional degradation phenomena have to be considered, as they occur under conditions of outdoor exposure[24–26]—a topic that we exclude here.

Nevertheless, since there are not only different corrosion mechanisms but also countless parameters that influence them (e.g., layer thickness, potential, substrate, etc.), it is difficult to predict the performance of different sample set-ups. Furthermore, the effects of these parameters are often interdependent, making it difficult to ascertain the extent of their impact when they vary. Various research groups have therefore been trying for a long time to determine the individual influencing factors on different corrosion mechanisms to predict how samples will perform under real conditions. Despite extensive efforts, the complete elucidation of the influence remains elusive, and research is ongoing.[6,27–29]

The starting point of this study was the observation that a commercial thermoset primer without a topcoat and as thin as 3 μm exhibited a superb resistance of more than 1000 h in a neutral SST. To identify the crucial parameters behind this excellent performance, a variety of coating variables (dry film thickness, polymeric matrix, substrate, pigments...) and accelerated laboratory corrosion tests have been employed, to elucidate the mode of action of thermoset primers without topcoats in a thickness range below 10 μm—a topic, which has gained up to now only little attention in the literature.[30–32]

Even though many publications exist that identify new testing methods and their advantages,[33–35] there are very few tests that are suitable and sufficient to represent the various mechanisms of damage.

The goal of this work is not to provide an overview of all the existing testing methods and describe our favorite ones, as previously done by Mills and Jamali.[36] Rather, our aim is to identify straightforward and easily accessible tests that can provide a comprehensive evaluation of individual sample performance while accounting for the effects of various factors. The selection of appropriate tests requires that they are complementary and capable of determining the influence of these factors.

Here, we decided to focus on neutral SSTs, including image analysis with and without the application of defined scribes (SST), cathodic delamination tests (CD), linear sweep voltammetry (LSV), and EIS, all of which have been well known for years and have been established in their field.[37–40] The combination of these five tests allowed us to evaluate the protection of the coatings against the most relevant damage mechanisms. In general, each test is suitable for assessing one or more parameters to yield an overall picture of the coating's

TABLE 1 Listing of all tests used and classification of which parameters are examined in each test.

| Testing method | Anodic delamination (AD) | Cathodic delamination (CD) | Barrier protection |
|---|---|---|---|
| Salt spray test (SST) without scribe | x | | x |
| SST with scribe | x | x | |
| Linear sweep voltammetry (LSV) | | | x |
| Electrochemical impedance spectroscopy (EIS) | | | x |
| CD | | x | x |

performance when combined. Table 1 presents an overview and the classification of the used tests.

Based on these tests, we benchmarked the performance of thin film primers across a set of varying engineering parameters such as thickness, wettability, and substrate. Additional characterization of the samples was performed using scanning electron microscopy (SEM) coupled with energy-dispersive X-ray spectroscopy (EDX).

We show that both layer thickness and type of substrate have the most significant influence on performance, while the primer formulation/chemistry is less important.

## 2 | MATERIALS AND METHODS

### 2.1 | Materials

For this study, two types of galvanized steel substrates in accordance with the standard DIN EN10346 were used, the exact compositions of which are listed in Table 2. The Z coatings consisted of an alloy of zinc and aluminum, ZM additionally also contained magnesium. The metallic coatings were fabricated by hot-dip galvanizing, and the surfaces were skin-pass rolled. All steel samples used in this study were supplied by voestalpine stahl GmbH.

Different primer formulations were used to distinguish various aspects of the primer formulations (e.g., hydrophopbizing, the inclusion of barrier pigments...). A list of the respective model primer components can be found in Table 3.

In addition, three commercially available primers based on polyester polyol binders and blocked trimeric isocyanate crosslinkers, were used (P1–P3). All commercial primers contained inhibitive pigments, that is, calcium-exchanged silica and possessed a peak metal temperature (PMT; temperature needed to completely crosslink the coating) of approximately 235°C and a dwell time of 25 s. A total of nine different primer formulations were the subject of this study.

TABLE 2 Composition and thickness of the metallic coatings on the used steel substrates.

| Label | Zn (%) | Al (%) | Mg (%) | Coating thickness (μm) | Total thickness (μm) |
|---|---|---|---|---|---|
| Z | 99.8 | 0.2 | - | 20 | 520 |
| ZM | 96 | 2.5 | 1.5 | 9 | 750 |

TABLE 3 Primer formulations used to determine the influence of hydrophobization and addition of barrier pigments.

| | S | HS | SM | SK | HSM | HSK |
|---|---|---|---|---|---|---|
| Polyester resin | 21.5 | 21.5 | 21.5 | 21.5 | 21.5 | 21.5 |
| Epoxy resin | 1.8 | 1.8 | 1.8 | 1.8 | 1.8 | 1.8 |
| Soft resin | 4.0 | 4.0 | 4.0 | 4.0 | 4.0 | 4.0 |
| Isocyanate | 5.0 | 5.0 | 5.0 | 5.0 | 5.0 | 5.0 |
| Defoamer | 0.3 | 0.3 | 0.3 | 0.3 | 0.3 | 0.3 |
| Silane | - | 2.5 | - | - | 2.5 | 2.5 |
| Shieldex C303 | 7.9 | 7.9 | 7.9 | 7.9 | 7.9 | 7.9 |
| Titanium dioxide TR 81 | 10.2 | 10.2 | 10.2 | 10.2 | 10.2 | 10.2 |
| ASP 400 | - | - | - | 4.5 | - | 4.5 |
| Plastorit micro | - | - | 4.5 | - | 4.5 | - |
| Aerosil R 972 | 0.3 | 0.3 | 0.3 | 0.3 | 0.3 | 0.3 |
| Methoxypropyl acetate | 29.0 | 26.5 | 30.0 | 30.0 | 27.0 | 27.0 |
| Solvesso 150 | 10.0 | 10.0 | 10.0 | 10.0 | 10.0 | 10.0 |
| Sum in wt.% | 90.0 | 90.0 | 95.5 | 95.5 | 95.0 | 95.0 |

### 2.2 | Coating application

The substrates were cleaned using an alkaline washing process to remove impurities and oil residues. The cleaning solution contained 10 g/L Bonderite C-AK C 72 (Henkel AG & CoKGaA) and was heated to 40°C during the process. Afterward, the clean substrates were treated with a chromium-free pretreatment solution (Bonderite 1455; Henkel AG CoKGaA) to gain a conversion layer, which provided additional

protection against corrosion and also acted as an adhesion promoter for the organic coating. The substrates were coated with primers using spiral-bar coaters of different thicknesses and then cured at the PMT of the respective material. To simulate the curing behavior of a primer-topcoat system, the specimens were cured for a second time at their respective PMT. The dry film thickness was measured using either the beta backscatter method (Fischerscope MMS, Fischer) or magnetoinductively (Deltascope FMP30, Fischer). Variations of ±1 µm were found with both measurement methods. No top coat was applied to the primers used in this study.

## 2.3 | Neutral SST

Neutral SST were performed in accordance with ISO 9227:2017. The specimens were cut to dimensions of 150 × 100 mm using plate shears. Two different experimental setups were used in this study. Undamaged samples were used to evaluate barrier properties. To check the protection against anodic delamination, two scribes were applied to the specimen surface: one down to the zinc coating and the other down to the steel substrate below. The edges of all the specimens were masked with adhesive tape to avoid the occurrence of inconclusive corrosion phenomena at the edges. The samples were photographed daily at the beginning and weekly thereafter to document the corrosion progress. After a defined time, all samples were removed from the chamber, and the status of the corroded or delaminated area was determined by evaluation using SMART, a commercial image analysis software package (http://www.quantiz.tech/). This software enables the detection of all color changes, allowing users to discern between intact and delaminated areas in recorded pictures.

## 2.4 | Electrochemical tests

All electrochemical measurements were performed in homemade measuring cells. For this purpose, PMMA tubes were glued to the primer surface to create an exposed surface area of approximately 12.5 cm², and the top of the tubes was covered. As electrolyte solution a 0.1 M NaCl solution was used, the contacted steel substrate acted as a working electrode, and a platinum mesh was used as a counter/reference electrode. The schematic representation of the setup is depicted in Figure 1a. The sample setup was connected to a potentiostat (Gamry Reference 600) and parameters were applied depending on the measurement performed.

Impedance measurements were conducted at the equilibrium OCP value that was measured after 24 h of contact of the sample with the electrolyte solution. The measured frequency range was $10^{-2}$ to $10^{5}$ Hz, and the excitation amplitude was 10 mV. EIS measurements were conducted every 120 min for 24 h to record the changes in the coating's impedance. To determine the linear polarization resistance (LPR), separate polarization curves in the range of ±10 mV versus the OCP were recorded every 120 min for 24 h after the electrolyte solution was added to the tube. The resistance was calculated using the slope in the range of ±5 mV versus the OCP of the polarization curves.

Regardless of the coating, the measured OCP value had adjusted to the value of the substrate in each experiment

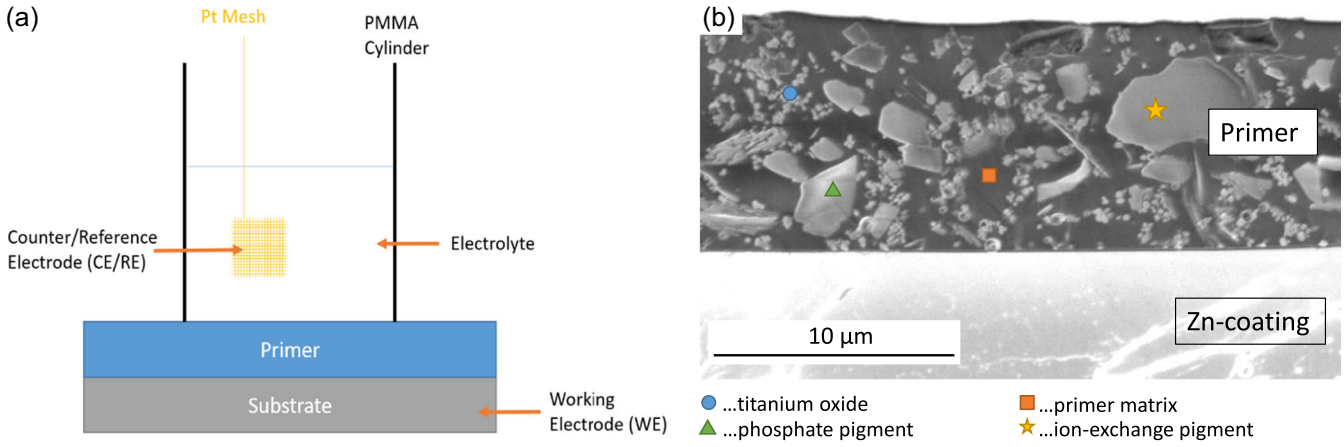


FIGURE 1 (a) Schematic illustration of the two-electrode setup used for the electrochemical measurements. (b) A cross-section polisher (CSP) cross section of a primer-coated sample on a hot-dip galvanized steel substrate with a zinc coating of approximately 20 µm per side (Z) before exposure to a salt spray test (SST). A commercially available primer with a layer thickness of approximately 9 µm was applied on top of the zinc coating. To identify the primer components, they were labeled with symbols. The square denotes the primer matrix, the circle titanium oxide, the triangle, a phosphate pigment, and the star an ion-exchange pigment. [Color figure can be viewed at wileyonlinelibrary.com]

after 24 h. The OCP value was −750 ± 10 mV versus SHE for the Z-samples and −783 ± 10 mV versus SHE for the ZM-samples. No differences were visible to the naked eye on the sample surface after the electrolyte exposure. EDX analyses showed no chemical differences, SEM images, however, showed small visual differences after electrolyte exposure, and the surface seemed a little rougher.

CD measurements were performed by simultaneously exposing up to eight samples, cut to 30 × 150 mm, to a constant current flow of 0.5 A in a 0.5 M KOH solution at 36°C for a defined period of time. The delaminated primer was removed in each case after the tests had been carried out using adhesive tape in accordance with ISO 2409:2013.

## 2.5 | Characterization

Cross-sectional images were acquired using a field-emission scanning electron microscope (SEM; Zeiss/Ultra 55) in conjunction with an energy-dispersive X-ray analyzer (EDX) to allow element identification and provide quantitative compositional information. The samples were prepared by cross-section polishing (CSP) using an argon ion beam. Figure 1b shows a typical cross-section in which the composition of the primer and the distribution of its components can be observed.

# 3 | RESULTS

All samples were characterized in various ways and then their performance was reviewed in different tests. Details on corrosion tests, electrochemical tests, and characterization can be found in Sections 2.3 to 2.5. Cross-sectional images of all samples were taken and the components were analyzed by EDX. These images can be used to visualize the arrangement of the primer system components. In combination with EDX, a microstructural characterization is also possible. Figure 2 shows the elemental analyses of various model primer samples containing classical and hydrophobized Shieldex pigments. In addition, either mica or kaolin was added as barrier pigments to the selected samples. No significant differences in the distribution of the pigments in the coating could be determined, which could be attributed to the low layer thickness. The average particle diameter of all pigments was ≤3.8 μm.

All specimens with intact surfaces that were exposed to the SST for 1000 h showed outstanding resistance to salt exposure (data not shown); almost all specimens appeared visually intact. This indicates that a thickness of 3 μm appears to be sufficient to provide protection against corrosion of the underlying substrate for a period of several weeks in SST. The barrier protection of the primer coating seems to be present even at a lower film thickness.

To further determine the influence of the substrate and pigments in the primer on the protection against anodic delamination, SSTs were subsequently performed with defects in the coating. Therefore, two scribes were applied to each of the specimens, one on the left-hand side down to the zinc coating and one on the right-hand side down to the underlying steel substrate in accordance with ISO 17872:2007.

In the first experiment, samples coated only with a clearcoat were compared with samples coated with

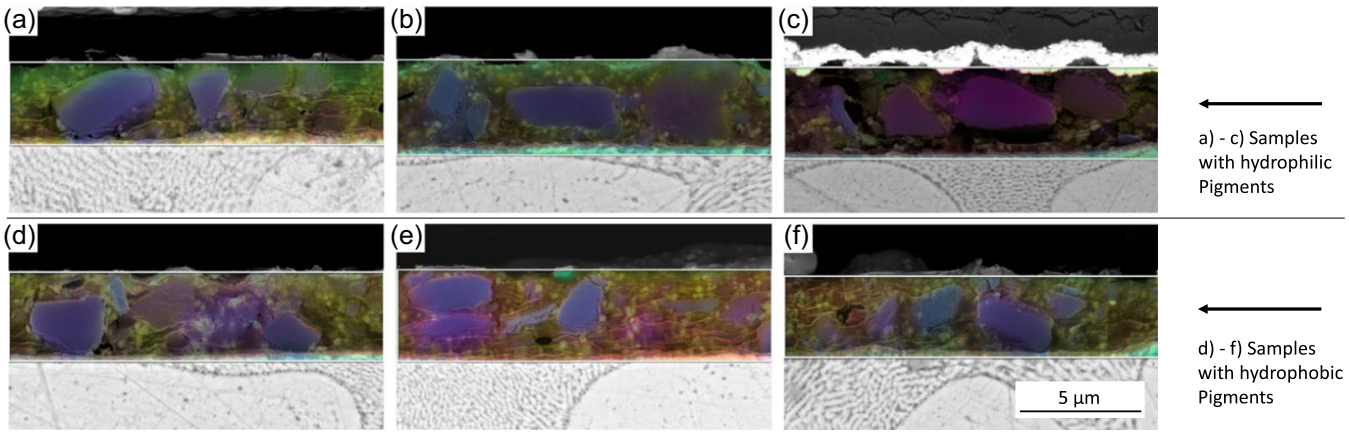


FIGURE 2 Scanning electron microscope images of the cross sections of the model primer samples. (a) with Shieldex only, (b) with Shieldex and mica, and (c) with Shieldex and kaolin. (d) with hydrophobized Shieldex only, (e) with hydrophobized Shieldex and mica, (f) with hydrophobized Shieldex and kaolin. All samples also contained titanium dioxide. The elements are highlighted in the following colors: titanium in yellow, silicon in purple, oxygen in blue, carbon in red, and calcium in green. No differences in pigment distribution were observed. The primer layer thickness was always approximately 3 μm. [Color figure can be viewed at wileyonlinelibrary.com]

primers containing only barrier pigments and with primers containing only inhibitive pigments. The model primers containing only inhibitive pigments performed consistently better than those containing only barrier pigments (data not shown).

In a more comprehensive set, different pigment variations, as well as a combination of pigments with different modes of action, were combined. More precisely, an inhibitive pigment (Shieldex) was used both in its original form (S) and hydrophobized form (HS), and each was used alone and in combination with two different barrier pigments, mica (M) and kaolin (K). To test the influence of the substrate, classic hot-dip galvanized steel (Z) as well as steel with a zinc magnesium aluminum coating (ZM) were used (details see methods and materials).

Figure 3a shows the results for this set after 672 h (for Z) and 2000 h (for ZM) in the SST. Because specimens with a ZM coating withstand exposure in the SST better than steel specimens with a Z coating, a longer residence time in the test chamber had to be selected to allow a meaningful evaluation and differentiation.[41,42] Blistering was only recognizable on the Z-samples; for the specimens with ZM coating, only corrosion was visible at the scribes. This strong effect can be attributed to the substrate.

To further quantitatively determine the delamination of the primer, the detached primer was carefully removed using a blunt scalpel, and the distance of detachment was calculated starting from the scribes using SMART software. Figure 3b shows the evaluation of delamination on Z-coated sample as well as on the ZM-coated samples in terms of the average delamination length.

For verification purposes, the samples were also examined by a white-light interferometer to determine the height differences between the primer surface and detached areas. Figure 4a displays a typical evaluation of a Z-coated sample. The height profile clearly shows that primer delamination eventually was anodic, that is, due to the dissolution of the zinc coating, causing the primer to lose its adhesion. Figure 4b depicts a cross-section recorded using a light microscope, in which this phenomenon can also be seen clearly.

The tests performed showed that as soon as artificial coating defects, in this case scribes, are applied to the zinc coating or the underlying steel substrate, delamination occurs. Galvanic effects within the scratch play a role, as the delamination from the scratches to the steel substrate is more pronounced than that from the scratches to the zinc layer. Under these conditions, mainly anodic contributions were observed—the metallic coating was completely dissolved under the delaminated coating, as can be seen in Figure 4b.

However, differences were observed between different substrates. Spherical irregularities occurring around the scribe on samples with a Z-coating indicate local cathodic delamination in the form of blistering at an earlier stage of the SST, whereas delamination on substrates with ZM-coatings occurred by the formation and propagation of corrosion products around the scribes. This can be attributed to the fact that ZM-coatings, in contrast to Z-coatings, form corrosion products that prevent oxygen reduction on the sample surface.[41,43] As a result, due to the potential gradient between the defect and the undamaged interface, cathodic delamination is not possible with ZM. Instead, delamination happens via an anodic mode that is triggered by ion migration at the metal oxide/polymer interface. Although being slower compared to Z coatings, the rate of delamination under prolonged exposure to the SST is not insignificant.[44] However, the corrosion of

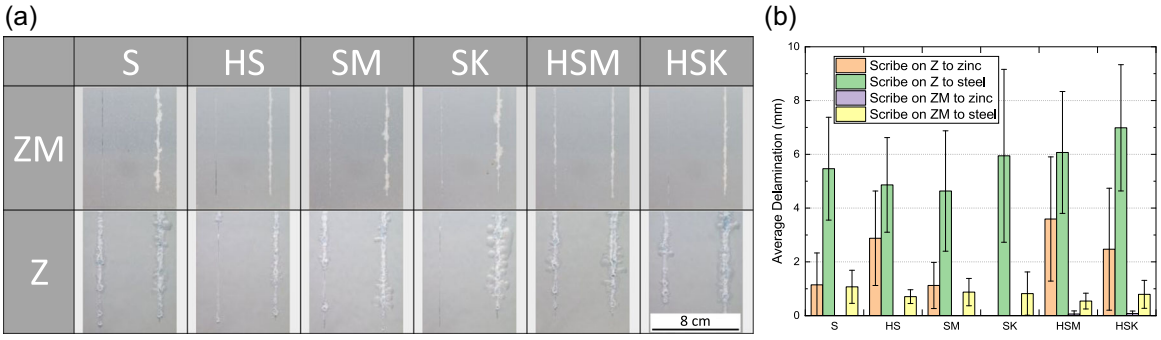


FIGURE 3 (a) Delamination and corrosion of model primers starting from the scribes on substrates with a pure zinc coating (Z) and samples with zinc-magnesium-aluminum coating (ZM) after 672 h (for Z) and 2000 h (for ZM) exposure. S contains only Shieldex, HS hydrophobized Shieldex, SM and SK in addition to Shieldex also mica and kaolin, respectively, HSM and HSK contain in addition to hydrophobized Shieldex also mica and kaolin, respectively. The size of the sample panels was 100 × 150 mm. The primer film thickness of all the samples was 3 μm. (b) Evaluation of scribe delamination of the model primers on Z and on ZM. [Color figure can be viewed at wileyonlinelibrary.com]

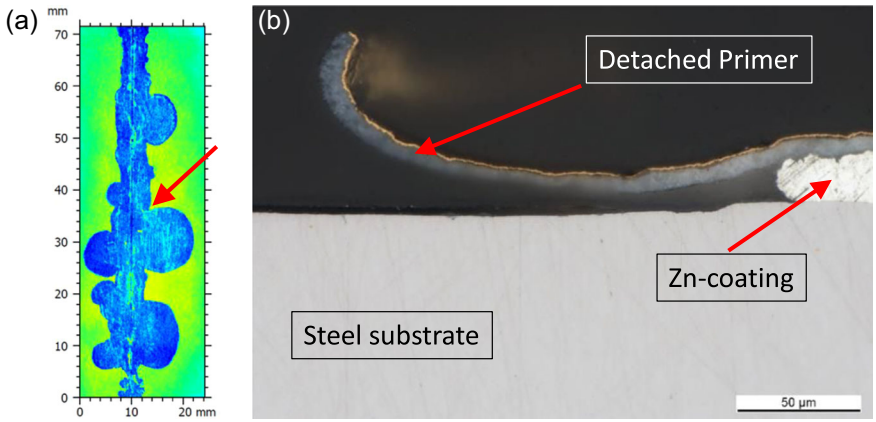


**FIGURE 4** (a) The type of delamination was determined by creating a height profile of the samples exposed to the salt-spray test using a white-light interferometer. The arrow indicates the position at which the cross-section was taken. (b) An optical microscope image of the cross-section of the transition area between the delaminated and still adhering primer. The predominance of the anodic delamination mechanism is evident. [Color figure can be viewed at wileyonlinelibrary.com]

the ZM-samples was similarly pronounced regardless of the primer formulation. In this test setup, making the pigments hydrophobic had hardly any effect on the scribes down to the steel substrate; albeit, it led to a deterioration on the scribes down to the zinc coating on average. We suspect that the hydrophobic treatment slowed the dissolution kinetics of the pigments, and thus reduced the protective effect, as part of the protective mechanism is the dissolution of the pigment.[45]

No clear statement can be made regarding the addition of barrier pigments. In the next step, provoked CD tests (see Section 2) were performed and the respective test durations were chosen to allow for optimal differentiation between the sample setups. The delaminated primer was removed in each case after the tests had been carried out using adhesive tape in accordance with ISO 2409:2013.

In these experiments, the addition of barrier additives (mica and kaolin) worsened the protection against cathodic delamination. This could be due to the creation of additional diffusion pathways caused by the nonoptimized formulation of the primers. The hydrophobization of the inhibition pigments significantly increased the resistance to delamination. This effect was particularly evident when comparing the primer samples that contained only Shieldex (S) with those that contained hydrophobic Shieldex (HS) on ZM. Hydrophobicity seemed to be decisive for the performance in this test.

Figure 5a displays the results of primer composition variations on hot-dip galvanized steel and steel with ZM-coating, respectively, at a primer layer thickness of 3 µm. S contains only Shieldex, HS hydrophobized Shieldex, SM and SK in addition to Shieldex also mica and kaolin, respectively, HSM and HSK in addition to hydrophobized Shieldex also mica and kaolin, respectively. The percentage of detached primers was calculated using the commercially available image analysis software SMART. An overview is shown in Figure 5b.

In the EIS measurements carried out to determine the barrier properties, the influence of the pigments could be determined more strongly than in the other tests. The hydrophobization of the inhibition pigments increased the impedance value, similar to the change from a Z-coating to a ZM-coating on the steel substrate. The latter tends to corrode faster, with the resulting corrosion products forming a protective layer that increases the measured impedance value. The addition of the barrier pigments mica and kaolin does not allow any clear statement regarding the influence on the measured impedance value, possibly because the formulation for the addition of mica/kaolin was not optimally selected. Figure 8a shows the measured impedance values at 100 mHz for the different primer formulations on both substrates.

While previous tests highlighted the influence of the substrate, we further tested the influence of the primer layer thickness on the performance of the samples in various tests. First, we examined the performance of the samples in the SST with scribed samples. To accomplish this, pretreated hot-dip galvanized steel substrates (Z) were coated with four different primers with film thicknesses of 3, 6, and 9 µm. The primers used were a model primer containing hydrophobized inhibitive pigments (HS), two commercially available thin-film primers with classical inhibitive pigments (P1 and P2), and a commercially available thick-film primer also containing classical inhibitive pigments (P3). These primers do not

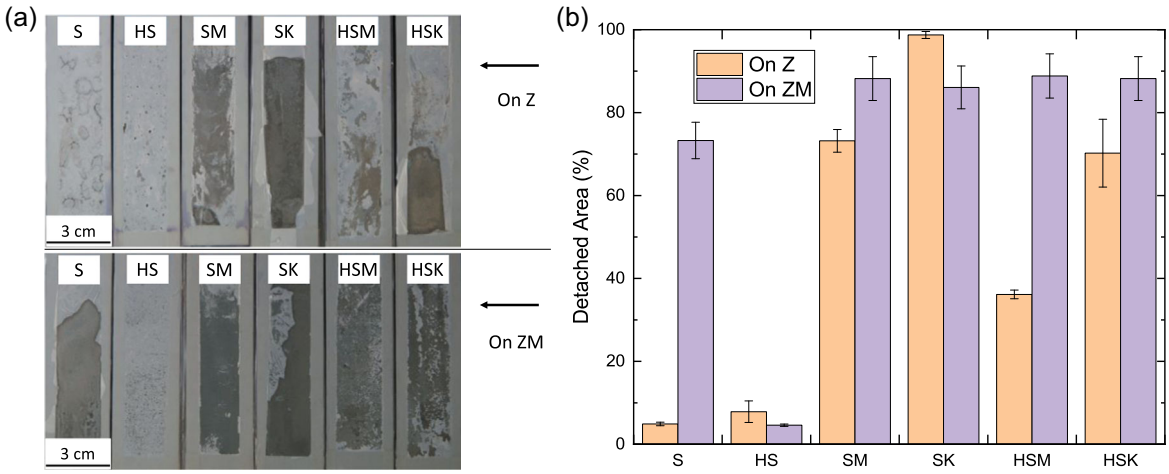


FIGURE 5 Comparison of the cathodic delamination of the model primers after 5 min. (a) Hot-dip galvanized steel with Z-coating (upper half) and hot-dip galvanized steel with ZM-coating (lower half). S contains only Shieldex, HS hydrophobized Shieldex, SM and SK in addition to Shieldex also mica and kaolin, respectively, HSM and HSK in addition to hydrophobized Shieldex also mica and kaolin, respectively. The primer film thickness of all samples was 3 μm. The delaminated primer was removed in each case after the tests were performed using adhesive tape, in accordance with ISO 2409:2013. (b) Overview of the percentages of detached primers using the image evaluation software SMART. [Color figure can be viewed at wileyonlinelibrary.com]

contain any hydrophobic pigments, so they come closest to the model primers S, SM, or SK. Figure 6a shows an overview matrix of all the specimen setups after 840 h of exposure in the SST, where the detached primer was carefully removed with a blunt scalpel.

Figure 6b shows the evaluation of the delamination using the SMART software for the delamination starting from the scribe to the zinc coating, as well as for the delamination starting from the scribe to the underlying steel. Different formulations with the same layer thickness are taken together in Figure 6c to better emphasize the effect of layer thickness.

As can be seen, the influence of the film thickness was clearly recognizable; therefore, not only differentiation between the various primer mixtures but also between the film thicknesses was possible. Furthermore, a correlation between the coating thickness of the applied primer and the protection against delamination was observed: the thicker the coating, the lower the delamination. None of the primers used proved to be superior to the others, and there was no correlation in the results of delamination at scribes down to the zinc coating, with delamination at scribes down to the steel substrate.

The increase in delamination from 3 to 6 μm is greater than that from 6 to 9 μm; a minimum layer thickness is presumably essential to provide stable protection against (water) diffusion, which is required for the electrochemical process. This is due to the size of the pigments, and likely due to less effective diffusion pathways along the coating, once the coating is considerably thicker compared to the pigment dimensions.

Figure 7 shows the results of the cathodic delamination test for the same set of samples. The percentage of detached primers was calculated using the commercially available image analysis software SMART. In Figure 7a, the results are sorted by primer and layer thickness, and in Figure 7b, the same layer thicknesses of different primers are summarized and presented as a box plot.

In summary, increasing the film thickness correlates positively with protection from delamination. However, even 9 μm is insufficient to ensure complete protection against delamination over longer test periods. Adhesion, and thus protection against delamination, is better on a ZM-coated substrate than on a Z-coated substrate.

Electrochemical measurements, including EIS, were also carried out to further complement the data above by assessing the polarization resistance. At the selected frequency of 100 mHz, the impedance is largely made up of the polarization resistance, which is also known as the (charge) transfer resistance. Another electrochemical method for determining the polarization resistance is linear voltammetry (LSV). In this case, the slope of the straight line of the linear area around the OCP is determined. Both methods, EIS and LSV, were performed and the results were compared. Figure 8b,c shows the data for different primer layer thicknesses of both methods side by side. In Figure 8b, the measurement data are sorted by type of primer, and in Figure 8c by layer thickness.

When the layer thickness is varied, a direct correlation between thickness and measured resistance value is

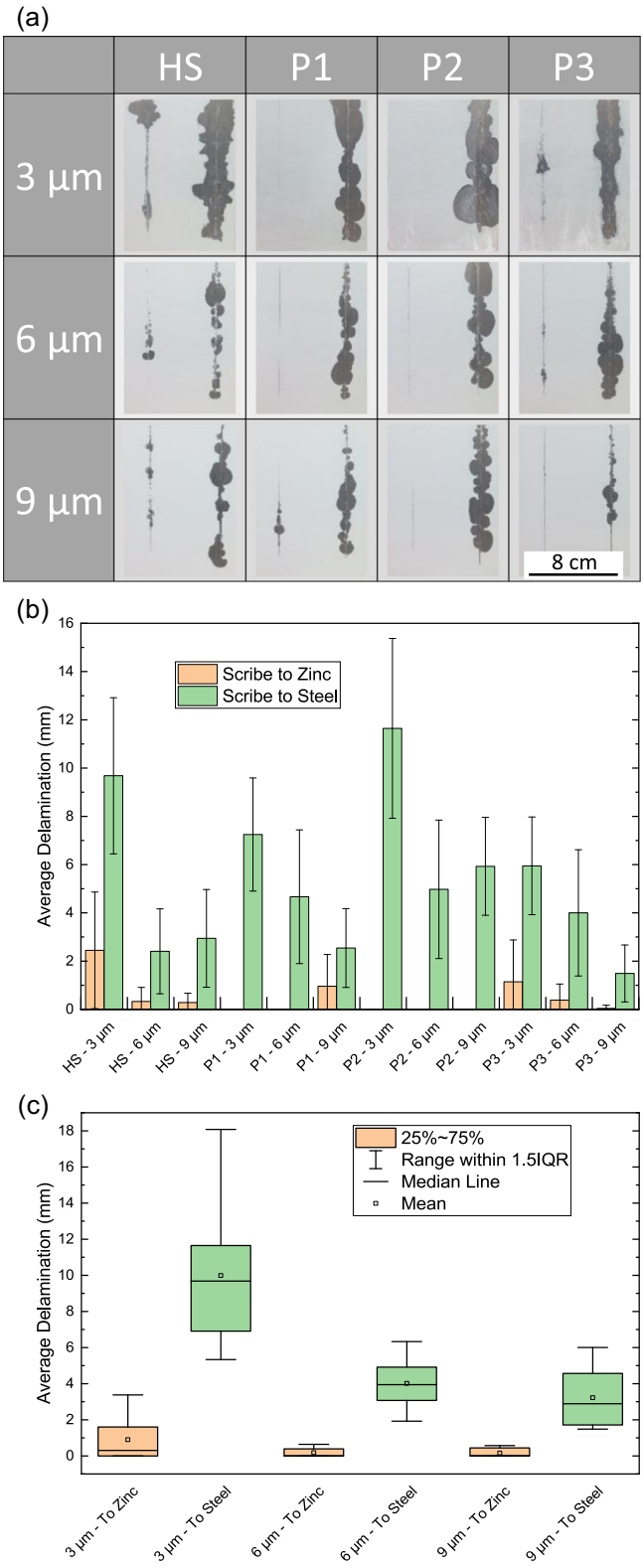


**FIGURE 6** (a) Result matrix of primer delamination starting from the scribes (left scribe down on the zinc coating, right scribe down to the steel substrate below) after 840 h of salt-spray test. HS was a model primer, P1 and P2 were commercially available thin-film primers, and P3 was a commercially available thick-film primer. All the primers were tested with different layer thicknesses (3, 6, and 9 µm) on zinc-coated steel (Z). The size of the sample panels was 100 × 150 mm. (b) Evaluation of the delamination of the film thickness variations of the four primers after 840 h in one image using the image evaluation software SMART. (c) Comparison of delamination at different layer thicknesses. [Color figure can be viewed at wileyonlinelibrary.com]

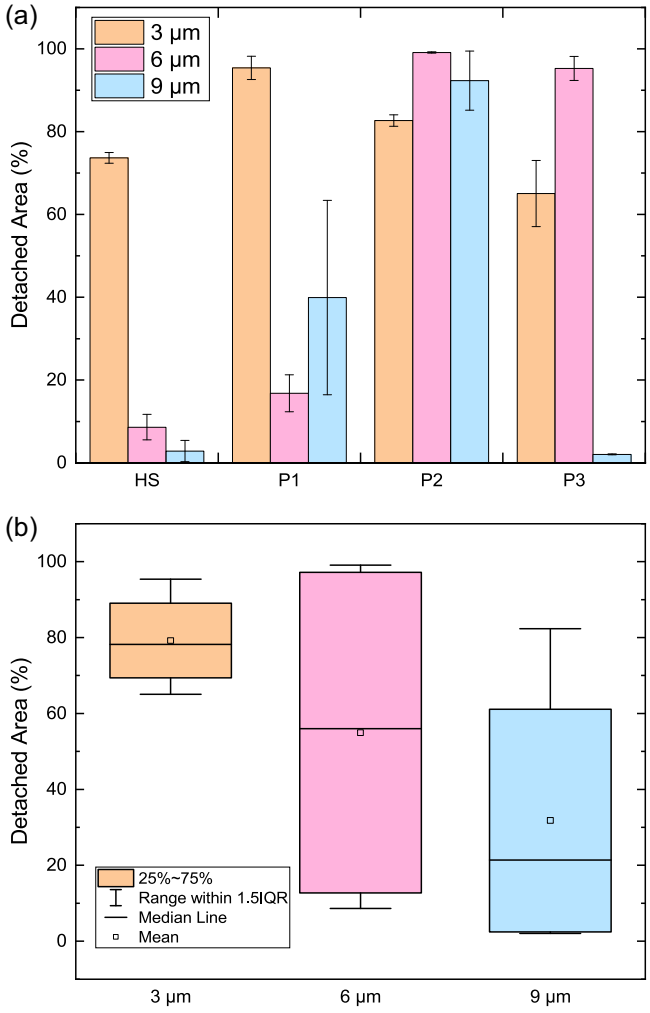


FIGURE 7 An overview of the percentage of detached primer from various specimen setups after cathodic delamination testing. The test duration was 10 min. Removal of the primer was done with adhesive tape according to ISO 2409:2013. HS denotes a model primer with hydrophobized Shieldex pigments, P1 and P2 denote commercially available thin-film primers, and P3 denotes a commercially available thick-film primer. All primers were applied with film thicknesses of 3, 6, and 9 µm. (a) sorted by primer and (b) sorted by film thickness. [Color figure can be viewed at wileyonlinelibrary.com]

obtained, regardless of the method used to determine the polarization resistance. However, there were large variations in the measurements of samples with the same layer thickness. Again, the influence of the layer thickness on the measured polarization resistance seems to be greater than that of the primer composition, as shown in Figure 8.

## 4 | DISCUSSION

In this work, we attempted to characterize a broad sample matrix of thin film primers using a limited but comprehensive set of standard corrosion tests to gain a better insight into the corrosion protection mechanisms of these systems. After careful consideration, we have chosen a range of five well-established tests that are in widespread use in many laboratories. The selected corrosion tests were employed as they represent the most frequently occurring failure mechanisms, that is, loss of barrier properties and anodic as well as cathodic coating delamination. A total of nine primer formulations without a topcoat have been tested in a layer thickness range of 3–9 µm on two different HDG substrates (Z and ZM).

With full integrity of the coating film, a 3 µm dry film thickness is already sufficient to obtain full corrosion protection for 1000 h in the SST—this was true for all investigated coating systems. As soon as artificial coating failures (i.e., scribing down to zinc or steel) are introduced, anodic delamination is prevalent, with significant contributions from the type of metallic coating (Z > ZM) and galvanic effects within the scribe (down to steel > down to zinc). No cathodic contributions were observed under these conditions as the metallic coating was completely dissolved under the delaminated coating (Figure 4). However, spherical irregularities around the scribe indicate blister formation (i.e., local cathodic delamination) at an earlier stage of the SST. EIS and LSV measurements were performed to determine the barrier properties. The resulting polarization resistances were in good agreement and were dominated by the dry film thickness, whereas the paint formulation played a minor role. EIS measurements further revealed that the pigments have an impact on the impedance value, with hydrophobic inhibition pigments and ZM coatings exhibiting higher impedance values compared to Z coatings. However, the addition of barrier pigments such as mica and kaolin does not yield a clear correlation with the impedance value, suggesting that the formulation for their addition may not have been optimally selected (Figure 8).

When the pigments in the primers were varied, organic coatings with a hydrophobic anticorrosive pigment possessed a higher polarization resistance and performed better in regard to protection against cathodic delamination than those formulations containing their nonhydrophobic counterparts. This can be attributed to the better adhesion of the primer due to the silanization of the pigments, as already described in the literature.[45] However, on average, primer formulations containing hydrophobic pigments underperformed their nonhydrophobic counterparts. We suspect that this is due to the slower reaction kinetics of the pigment dissolution, caused by the hydrophobic treatment, which may form a barrier on the pigment. Hence, leaching and the subsequent exchange process are slowed down, and corrosion is less effectively inhibited. Furthermore, the

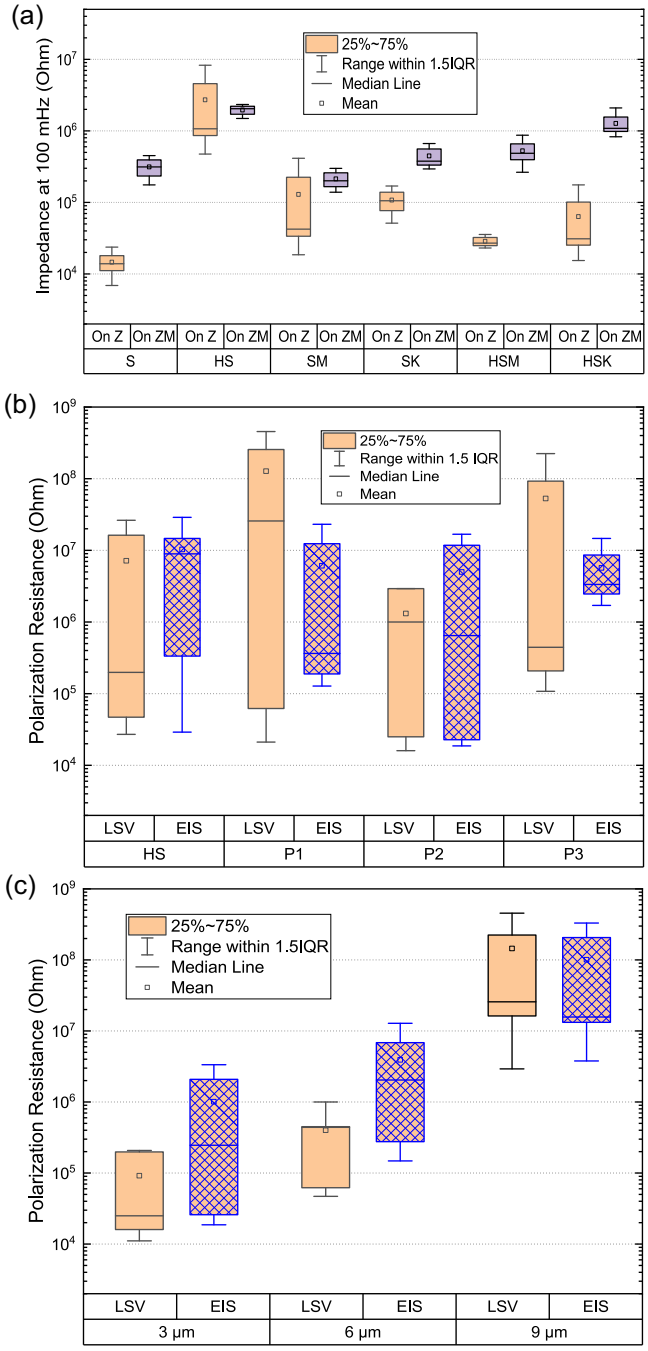


**FIGURE 8** (a) Measured impedance values at 100 mHz after 24 h exposure to a 1 M NaCl solution of 3 µm thick model primer coatings on substrates with pure zinc coating and substrates with Zn-Al-Mg coating. S contains only Shieldex, HS hydrophobized Shieldex, SM and SK in addition to Shieldex also mica and kaolin, respectively; HSM and HSK in addition to hydrophobized Shieldex also mica and kaolin, respectively. (b) Comparison of the measured polarization resistances from polarization measurements using linear sweep voltammetry (LSV) (black frame) and electrochemical impedance spectroscopy (EIS) using the impedance values at 100 mHz (blue frame) when varying the film thicknesses of different commercial primers (P1–P3) sorted by the type of primer; (c) the same measurements sorted by primer thickness. [Color figure can be viewed at wileyonlinelibrary.com]

addition of barrier pigments (kaolin or mica) did not result in a clear improvement in the performance in any of the tests.

In general, and irrespective of the formulation, increasing the layer thickness resulted in an improvement in the performance in all tests, regardless of the primer formulation. By varying various parameters, we were able to determine that the layer thickness, in particular, via the barrier effect and selection of the substrate, had a significant influence on the protection against corrosion.

The selection of the composition (binders, fillers, pigments, etc.) also plays a role but is overpowered by the choice of substrate and layer thickness.

Generally speaking, it is difficult to predict how the samples will perform in real-world conditions, considering that all parameters interact. However, it is possible to rank different samples when evaluating individual parameters, thereby assessing the samples' suitability for different applications.

## 5 | CONCLUSIONS

In this work, we aimed to understand the influence of individual factors such as coating thickness, composition, and substrate on the corrosion resistance of galvanically protected steel sheets that were coated with thin film primers only. The test programs of this work indicate that the thin film thickness and type of substrate have a strong influence on performance and to a lesser degree the primer formulation/chemistry.

These are the main conclusions of this work:

- With full integrity of the coating film, 3 µm dry film thickness are already sufficient to obtain full corrosion protection for 1000 h in the SST, while the thickness of coatings has a strong influence once damage is present.
- Increasing the film thickness improves the performance in every test, regardless of the primer composition, except for the SST tests without scribes, where 3 µm is sufficient for full protection and there is no additional benefit to increasing the film thickness.
- Hydrophobization of Shieldex reduces the efficiency of pigments, which improves the performance in the cathodic delamination test, whereas it has a negative effect on the protection against white rust formation. We suspect that this is due to the fact that the hydrophobic treatment slows down the leaching of the pigments and thus the ion exchange, which reduces the protective function in the SST. On the other hand, silanization improves adhesion and thus also protects against cathodic delamination.

These results help to advance the optimization of thin-film primers, however, further research is needed to fully understand their potential in practical applications. Specifically, future studies could evaluate the performance of these coatings in real-world environments, such as marine or industrial settings, and monitor the corrosion resistance of samples over time while considering different environmental conditions like UV radiation and humidity. Further investigation into the effect of hydrophobization on corrosion resistance is also warranted, as it had differing effects on cathodic delamination and protection against white rust formation.

Overall, this work demonstrates that competing effects can be traced well using the combination of the suggested five corrosion tests, and targeted engineering of thin film primers becomes possible. We recommend that practitioners and researchers consider our findings in the development of improved thin-film primers for corrosion protection in various applications.

## ACKNOWLEDGMENTS

The authors acknowledge the support from all members of the department "Corrosion protection and organic coatings" and the department "Technical service test center B" at voestalpine Stahl GmbH. The authors thank Voestalpine Stahl GmbH for providing the materials used for the work. The authors acknowledge TU Wien Bibliothek for financial support through its Open Access Funding Program. Open access funding provided by KEMO - Technische Universitat Wien.

## CONFLICT OF INTEREST STATEMENT

The authors declare no conflict of interest.

## DATA AVAILABILITY STATEMENT

Research data are not shared.

## ORCID

*Simon Wiener* http://orcid.org/0000-0003-3294-9635

## REFERENCES

[1] F. Presuel-Moreno, M. A. Jakab, N. Tailleart, M. Goldman, J. R. Scully, *Mater. Today* **2008**, *11*, 14.
[2] N. Priyantha, P. Jayaweera, A. Sanjuro, K. Lau, F. Lu, K. Krist, *Surf. Coat. Technol.* **2003**, *163*, 31.
[3] Y. Shi, B. Yang, P. K. Liaw, *Met.* **2017**, *7*, 43.
[4] A. E. Hughes, *Encyclopedia of Interfacial Chemistry*, Elsevier, Amsterdam **2018**.
[5] A. Zaki, *Principles of Corrosion Engineering and Corrosion Control*, Butterworth-Heinemann, Oxford (UK) **2006**.
[6] O. Ø. Knudsen, A. Forsgren, *Corrosion Control Through Organic Coatings*, CRC Press, Boca Raton **2017**.
[7] S. B. Lyon, R. Bingham, D. J. Mills, *Prog. Org. Coat.* **2017**, *102*, 2.
[8] P. A. Sørensen, S. Kiil, K. Dam-Johansen, C. E. Weinell, *J. Coat. Technol. Res.* **2009**, *6*, 135.
[9] M. Ström, *Presented at EUROCORR* **2014**, Pisa.
[10] H. S. Gardner, *Cyclic Cabinet Corrosion Testing*, ASTM International, West Conshohocken **1995**.
[11] I. C. P. Margarit-Mattos, *Electrochim. Acta* **2020**, *354*, 136725.
[12] R. Montoya, F. R. García-Galván, A. Jiménez-Morales, J. C. Galván, *Corros. Sci.* **2014**, *82*, 432.
[13] K. Ogle, S. Morel, N. Meddahi, *Corros. Sci.* **2005**, *47*, 2034.
[14] W. Fürbeth, M. Stratmann, *Corros. Sci.* **2001**, *43*, 207.
[15] P. A. Sørensen, S. Kiil, K. Dam-Johansen, C. E. Weinell, *Prog. Org. Coat.* **2009**, *64*, 142.

[16] J. M. Pommersheim, T. Nguyen, *Organic Coatings for Corrosion Control*, American Chemical Society, Washington, DC **1998**.
[17] R. P. Berkelaar, P. Bampoulis, E. Dietrich, H. P. Jansen, X. Zhang, E. S. Kooij, D. Lohse, H. J. W. Zandvliet, *Langmuir* **2015**, *31*, 1017.
[18] A. S. Kuznetsov, M. A. Gleeson, F. Bijkerk, *J. Phys. Condens. Matter* **2012**, *24*, 052203.
[19] J. W. Martin, E. Embree, W. Tsao, *J. Coat. Technol.* **1990**, *62*, 25.
[20] M. Kendig, *Corrosion* **1992**, *48*, 218.
[21] H. Leidheiser, W. Funke, *J. Oil Colour Chem. Assoc.* **1987**, *70*, 121.
[22] M. Van Loo, D. D. Laiderman, R. R. Bruhn, *Corrosion* **1953**, *9*, 277.
[23] R. T. Ruggeri, T. R. Beck, *Corrosion* **1953**, *39*, 452.
[24] F. Deflorian, S. Rossi, M. Fedel, *Corros. Sci.* **2008**, *50*, 2360.
[25] F. Deflorian, S. Rossi, L. Fedrizzi, C. Zanella, *Prog. Org. Coat.* **2007**, *59*, 244.
[26] X. Yong, H. Ji, Z. Chen, X. Ruan, *J. Electrochem. Soc.* **2021**, *168*, 121506.
[27] S. G. R. Emad, X. Zhou, S. B. Lyon, G. E. Thompson, Y. Liu, G. Smyth, D. Graham, D. Francis, S. R. Gibbon, *Prog. Org. Coat.* **2017**, *102*, 71.
[28] F. Mahdavi, M. Forsyth, M. Y. J. Tan, *Prog. Org. Coat.* **2017**, *103*, 83.
[29] S. G. Croll, *Prog. Org. Coat.* **2020**, *148*, 105847.
[30] M. E. McMahon, R. J. Santucci, Jr., C. F. Glover, B. Kannan, Z. R. Walsh, J. R. Scully, *Front. Mater. Sci.* **2019**, *6*, 190.
[31] U. Rammelt, P. T. Nguyen, W. Plieth, *Electrochim. Acta* **2001**, *46*, 4251.
[32] E. Jaehne, S. Oberoi, H.-J. P. Adler, *Prog. Org. Coat.* **2008**, *61*, 211.
[33] X. Chen, C. Shaw, L. Gelman, K. T. V. Grattan, *Measurement* **2019**, *139*, 387.
[34] S. Mabbutt, D. J. Mills, C. P. Woodcock, *Prog. Org. Coat.* **2007**, *59*, 192.
[35] P. A. White, G. E. Collis, M. Skidmore, M. Breedon, W. D. Ganther, K. Venkatesan, *New J. Chem.* **2020**, *44*, 7647.
[36] D. J. Mills, S. S. Jamali, *Prog. Org. Coat.* **2017**, *102*, 8.
[37] N. LeBozec, N. Blandin, D. Thierry, *Mater. Corros.* **2008**, *59*, 889.
[38] V. Lavaert, M. Moors, E. Wettinck, *J. Appl. Electrochem.* **2002**, *32*, 853.
[39] R. M. Souto, M. L. Llorente, L. Fernández-Mérida, *Prog. Org. Coat.* **2005**, *53*, 71.
[40] F. Mahdavi, M. Forsyth, M. Y. J. Tan, *Prog. Org. Coat.* **2017**, *105*, 163.
[41] M. S. Azevedo, *PhD Thesis*, Université Pierre et Marie Curie, Paris, **2014**.
[42] T. A. Keppert, G. Luckeneder, K.-H. Stellnberger, C. Commenda, G. Mori, H. Antrekowitsch, *Mater. Corros.* **2014**, *65*, 871.
[43] T. A. Keppert, G. Luckeneder, K.-H. Stellnberger, G. Mori, H. Antrekowitsch, *Mater. Corros.* **2014**, *65*, 560.
[44] R. Hausbrand, M. Stratmann, M. Rohwerder, *Corros. Sci.* **2009**, *51*, 2107.
[45] T. Fletcher, *JCT Coatingstech* **2013**, *10*, 28.

**How to cite this article:** S. Wiener, B. Strauß, G. Luckeneder, J. Hagler, M. Valtiner, *Mater. Corros.* **2023**, 74, 1183–1195.
https://doi.org/10.1002/maco.202313786